International Journal of Pure and Applied Mathematics
Volume 63 No. 2 2010, 183-195

MODELING OF TWO-FLUID FLOW AND HEAT TRANSFER WITH SOLIDIFICATION IN CONTINUOUS STEEL CASTING PROCESS UNDER ELECTROMAGNETIC FORCE

T. Mookum[1], B. Wiwatanapataphee[2] §, Y.H. Wu[3]
[1,2]Department of Mathematics
Faculty of Science
Mahidol University
272, Rama 6 Road, Rajthevee, Bangkok, 10400, THAILAND
[2]e-mail: scbww@mahidol.ac.th
[3]Department of Mathematics and Statistics
Curtin University of Technology
Perth, WA 6845, AUSTRALIA
e-mail: yhwu@maths.curtin.edu.au

Abstract: This paper is concerned with the two-fluid flow and heat transfer in the continuous steel casting process under electromagnetic (EM) force. The governing equations consist of the Navier-Stokes equations, the continuity equation, and the energy equation. The influence of the EM field on the flow pattern, the meniscus shape, and temperature distribution in the EM caster is modeled by the addition of the EM force and the surface tension force in the Navier-Stokes equations. The EM force is defined by the cross product of current density and magnetic flux density obtained from the Maxwell's equations. A surface tension force is a function of the level set function which can be solved from the level set equation. A complete set of governing equations is solved by the level set finite element method. The numerical results demonstrate that the EM field applied to the system has significant effect on the two-fluid flow, meniscus profile, and temperature distribution.

AMS Subject Classification: 35Q60, 74A50, 74F15, 74S05, 83C50
Key Words: electromagnetic stirring, continuous steel casting process, two-fluid flow, heat transfer, level set finite element method

Received: June 23, 2010

§Correspondence author

1. Introduction

In the continuous steel casting process, it has been recognized that most of surface defects occur around the meniscus region. Understanding of the complex phenomena around this region is important. These phenomena include two-fluid flow and heat transfer with solidification. Over the last decade, extensive studies have been carried out worldwide to model the fluid flow and steel solidification using the EM stirring, see [16, 19, 21]. By ignoring the meniscus behavior, the results obtained from those studies give basic understanding of the fluid flow and heat transfer. Recently, meniscus behavior has been studied by both experimental models and numerical models. In experimental models, [8] including water model, [6], water/air model [9], the results indicate that there are many parameters affecting the meniscus shape. The meniscus amplitude increases significantly when the inlet velocity increases, the port angle increases, or the immersion depth of submerge entry nozzle (SEN) decreases. By applying a magnetic field in the continuous casting, the meniscus always keeps the parabolic shape near the mould wall, see [8]. In computational models with EM effect, extensive studies have focused on the model of the heat transfer and single fluid flow. Very little attempt has been made to couple the heat transfer and two-fluid flow in EM continuous casting process. The meniscus may be regarded as the gradient of the magnetic pressure (see [10, 25]) and may be calculated by the action of Lorentz force, see [19, 11]. The results show that the meniscus height increases when the magnetic flux density and the frequency of magnetic field increase. In the computational models with no EM effect, the meniscus shape is calculated by the volume-tracking method, see [2, 18] and the Bikerman equation, see [14, 17]. The Bikerman equation can capture the meniscus shape only near the mould wall whereas the volume-tracking method can determine the meniscus shape in the mould. Another method that has been used widely to determine the interface between two fluids is the level set method. The level set method originally introduced by Osher and Sethian [13] is the most popular technique for solving two-fluid flow problems. This method is applied in several problems such as dam breaking (see [7, 23]), rising bubble (see [12, 22]), and droplet (see [20, 24]).

In this study, we propose a mathematical model for the problem of coupled two-fluid flow and heat transfer with solidification in the EM continuous steel casting process. A finite element based level set method is developed for simulating the coupled two-fluid flow, heat transfer and steel solidification phenomena. The effect of source current density on the meniscus shape, the flow of lubricant oil and molten steel, and solidification of steel is investigated. The

rest of the paper is organized as follows. In Section 2, a complete set of field equations is given. In Section 3, the method of solution is presented. Section 4 represents a numerical study to demonstrate the influence of source current density on the flow of two fluids, the meniscus shape, and the heat transfer with solidification.

2. Mathematical Model

In this work, we study the motion of the molten steel and lubricant oil, the meniscus shape, and the heat transfer with solidification in the EM continuous steel casting process. The molten steel and lubricant oil are assumed to be incompressible Newtonian fluid. The lubricant oil acting as thermal insulator is filled up on the top of the molten steel to protect the steel from oxidation. The governing equations describing the coupled two-fluid flow and heat transfer with solidification in the EM caster are the continuity equation, the Navier-Stokes equations, the energy equation, and the level set equation:

$$\nabla \cdot \mathbf{u} = 0, \tag{1}$$

$$\rho\left(\frac{\partial \mathbf{u}}{\partial t} + \mathbf{u}\cdot\nabla\mathbf{u}\right) - \nabla\cdot\left[-p\mathbf{I} + \mu(\nabla\mathbf{u} + (\nabla\mathbf{u})^T)\right] = \rho\mathbf{g} + \mathbf{F}_{em} + \mathbf{F}_{st}, \tag{2}$$

$$\rho c\left(\frac{\partial T}{\partial t} + \mathbf{u}\cdot\nabla T\right) = \nabla\cdot(k\nabla T) + Q_T, \tag{3}$$

and

$$\frac{\partial \phi}{\partial t} + \mathbf{u}\cdot\nabla\phi = 0, \tag{4}$$

where $\mathbf{u}, p, T$ and ϕ denote respectively the velocity field, pressure, temperature field, and level set function; ρ and μ are the density and viscosity of fluid; g is the gravitational acceleration; c and k are the heat capacity and thermal conductivity of the fluid.

The level set function in equation (4) is defined to be negative in the molten steel Ω_s, positive in the lubricant oil Ω_o, and zero level on the interface Γ_{int}:

$$\phi(\mathbf{x},t)\begin{cases} < 0 & \text{if } \mathbf{x}\in\Omega_s, \\ = 0 & \text{if } \mathbf{x}\in\Gamma_{int}, \\ > 0 & \text{if } \mathbf{x}\in\Omega_o, \end{cases} \tag{5}$$

Since the physical properties of the two fluids are different, they are discontinuous on the interface. To smooth the discontinuities, the density, viscosity, heat capacity, and thermal conductivity are represented in terms of the smooth

Heaviside function $H(\phi)$ as

$$\rho(\phi) = \rho_s + (\rho_o - \rho_s)H(\phi), \tag{6}$$

$$\mu(\phi) = \mu_s + (\mu_o - \mu_s)H(\phi), \tag{7}$$

$$c(\phi) = c_s + (c_o - c_s)H(\phi), \tag{8}$$

$$k(\phi) = k_s + (k_o - k_s)H(\phi), \tag{9}$$

where the subscripts s and o denote respectively the molten steel and lubricant oil and $H(\phi)$ is defined by

$$H(\phi) = \begin{cases} 0 & \text{if } \phi < -\varepsilon, \\ \dfrac{1}{2}\left[1 + \dfrac{\phi}{\varepsilon} + \dfrac{1}{\pi}\sin\left(\dfrac{\pi\phi}{\varepsilon}\right)\right] & \text{if } |\phi| \le \varepsilon, \\ 1 & \text{if } \phi > \varepsilon, \end{cases} \tag{10}$$

for the small thickness of the interface ε, see [4, 15].

The EM force, $\mathbf{F}_{em}$, in equation (2) is determined by

$$\mathbf{F}_{em} = \mathbf{J} \times (\nabla \times \mathbf{A}), \tag{11}$$

where $\mathbf{A}$ and $\mathbf{J}$ are the magnetic vector potential and current density, respectively. Based on our previous work in [1], $\mathbf{A}$ and $\mathbf{J}$ can be determined by the following two equations:

$$\nabla \times (\frac{1}{\nu}\nabla \times \mathbf{A}) = \mathbf{J}, \tag{12}$$

$$\nabla \cdot (-\eta\nabla\varphi + \mathbf{J}_s) = 0, \tag{13}$$

where $\mathbf{J} = -\eta\nabla\varphi + \mathbf{J}_s$, ν and η denote respectively the magnetic permeability and electroconductivity, $\mathbf{J}_s$ is the source current density, φ is a scalar potential function. The surface tension force in equation (2) acting only at the interface can be expressed as

$$\mathbf{F}_{st} = \sigma\kappa(\phi)\delta(\phi)\hat{n}, \tag{14}$$

where σ is the surface tension coefficient, $\hat{n} = \frac{\nabla\phi}{|\nabla\phi|}$ is the unit normal on the interface, $\kappa(\phi) = -\nabla \cdot \hat{n}$ is the interfacial curvature, $\delta(\phi)$ is the delta function [3, 4]. In this study, the delta function for the simulation is chosen to be $\delta(\phi) = 6|\nabla\phi||\phi^2 - \alpha^2|$ for $\alpha = \frac{3}{2}\varepsilon$.

The heat source Q_T in equation (3) occurring only in the steel region represents the phase change and is zero everywhere except in the mushy region where

$$Q_T = -\rho_s\left(\frac{\partial H_L}{\partial t} + \mathbf{u} \cdot \nabla H_L\right)(1 - H(\phi)), \tag{15}$$

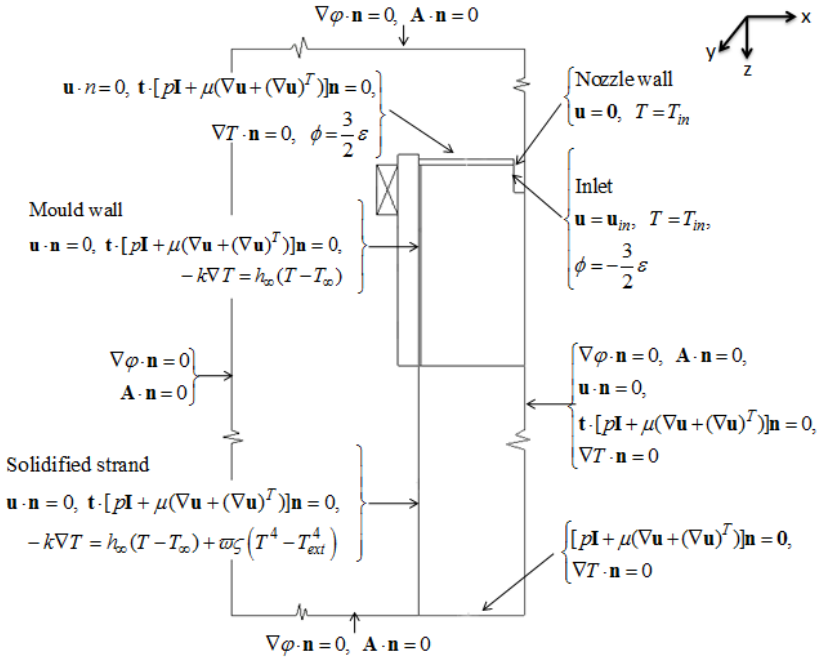

Figure 1: Boundary conditions

where H_L is the latent heat given by

$$H_L = Lf(T) = \begin{cases} 0 & \text{if } T \le T_S, \\ L\dfrac{T-T_S}{T_L-T_S} & \text{if } T_S < T < T_L, \\ L & \text{if } T \ge T_L, \end{cases} \tag{16}$$

in which L is the latent heat of liquid steel, $f(T)$ is the liquid fraction, T_S and T_L are the solidification temperature and melting temperature of the steel, respectively.

For two-dimensional problems, equations (1)-(16) with the boundary conditions as shown in Figure 1 can be manipulated to yield two closed systems of partial differential equations. One is a stable system for determining the EM field and another is an unstable system of five coordinate and time dependent unknown functions (u_1, u_2, p, T, and ϕ).

3. Method of Solution

In this study, we are concerned with two-dimensional cases. The EM field in the system of equations (12) and (13) is solved first to yield the EM force in equation (11) for subsequent two-fluid flow and heat transfer analysis (see more detail in paper [21]). The governing partial differential equations of unsteady unknown functions (u_1, u_2, p, T, and ϕ) are then discretized in space by the level set finite element method to yield the following system of nonlinear ordinary differential equations

$$M\dot{\mathbf{q}} + K\mathbf{q} = \mathbf{f}, \tag{17}$$

where $\mathbf{q}$ represents the values of the corresponding unknown $\mathbf{U}, \mathbf{P}, \mathbf{T}$, and Φ at the nodes of the finite element mesh. The matrix M corresponds to the transient terms in the governing partial differential equations, the matrix K corresponds to the advection and diffusion terms depends nonlinearly on $\mathbf{U}$ and Φ, and the vector $\mathbf{f}$ depends nonlinearly on $\mathbf{U}, \mathbf{T}$, and Φ.

The numerical solutions to the nonlinear discretization system with appropriate boundary conditions are then obtained by using an iterative scheme developed based on the Euler's backward scheme. The following convergent condition was used in the simulation

$$\|R_i^{m+1} - R_i^m\| \leq Tol, \tag{18}$$

where the subscripts $m+1$ and m denote iterative computation steps, R_i denotes the solution vector of the i-th variable on the finite element nodes, $\|\cdot\|$ is the Euclidean norm and Tol is a small positive constant.

4. Numerical Investigation and Discussion

The influence of the EM field on the coupled two-fluid flow and heat transfer solidification process is investigated in the present study. The example under investigation is a rectangular caster which has a width of 0.1 m and a depth 0.4 m in the $x - z$ plane. The computation domain as shown in Figure 2 was discretized using 14,927 triangular elements with a total of 128,941 degrees of freedom. The finer grid was used in the lubricant oil region and near the interface. The values of model parameters used in this simulation are as listed in Table 1.

Figure 3 shows the EM force $\mathbf{F}_{em}$ corresponding to different source current density J_s^e. The results show that the EM force acts on the molten steel in

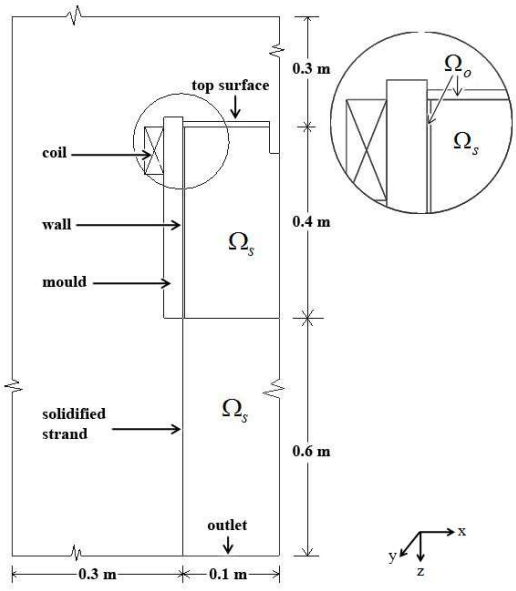

Figure 2: Computation domain Ω

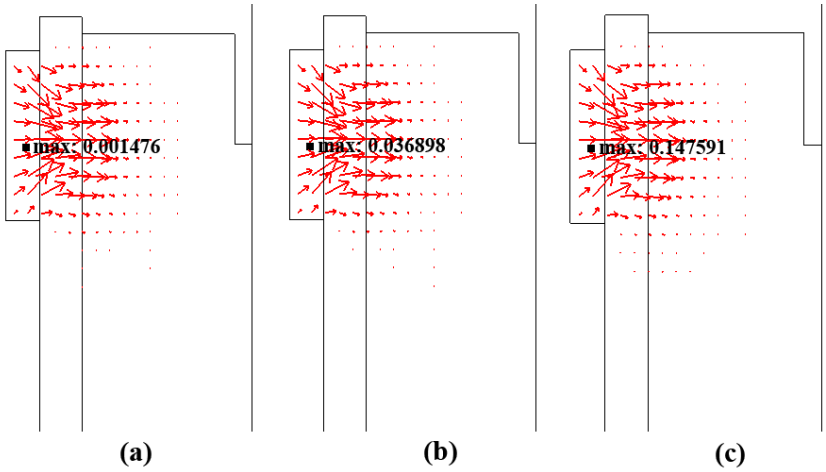

Figure 3: Influence of external current density J_s^e on the EM force (a) $J_s^e = 10^4 A/m^2$; (b) $J_s^e = 5 \times 10^4 A/m^2$; (c) $J_s^e = 10^5 A/m^2$

the horizontal direction toward the center line. This force will prevent the steel from sticking to the mould wall. The results also show that the magnitude of

Parameters	Value	Unit
Delivery velocity of molten steel U_{in}	0.012	m/s
Density ρ		
-molten steel	7800	kg/m^3
-lubricant oil	2728	kg/m^3
Effective viscosity μ		
-molten steel	0.001	$Pa \cdot s$
-lubricant oil	0.0214	$Pa \cdot s$
Surface tension coefficient σ	1.6	m/s^2
Thickness of the interface ε	0.001	m
Gravitational acceleration g	-9.8	m/s^2
Pouring temperature T_{in}	1535	^oC
Molten steel temperature T_L	1525	^oC
Solidified steel temperature T_S	1465	^oC
Ambient temperature T_∞	100	^oC
External temperature T_{ext}	100	^oC
Mould wall temperature T_m	1000	^oC
Heat capacity c		
-molten steel	465	J/kg^oC
-lubricant oil	1000	J/kg^oC
Thermal conductivity k		
-molten steel	35	W/m^oC
-lubricant oil	1	W/m^oC
Latent heat L	2.72×10^5	J/kg
Heat transfer coefficient of molten steel h_∞	1079	$W/m^{2o}C$
Emissivity of solid steel ϖ	0.4	
Stefan-Boltzmann constant ς	5.66×10^{-8}	W/m^2K^4
Magnetic permeability of vacuum ν	$4\pi \times 10^{-7}$	Henry/m
Electric conductivity η		
-molten steel	4.032×10^6	
-coil	1.163×10^6	
-air	10^{-39}	

Table 1: Parameters used in numerical simulation

the force increases as the current density increases. Figure 4 shows the influence of source current density on the velocity and temperature fields. The results indicate that the magnitude of source current density has a considerable effect on the flow and temperature fields. It is noted that a higher source current

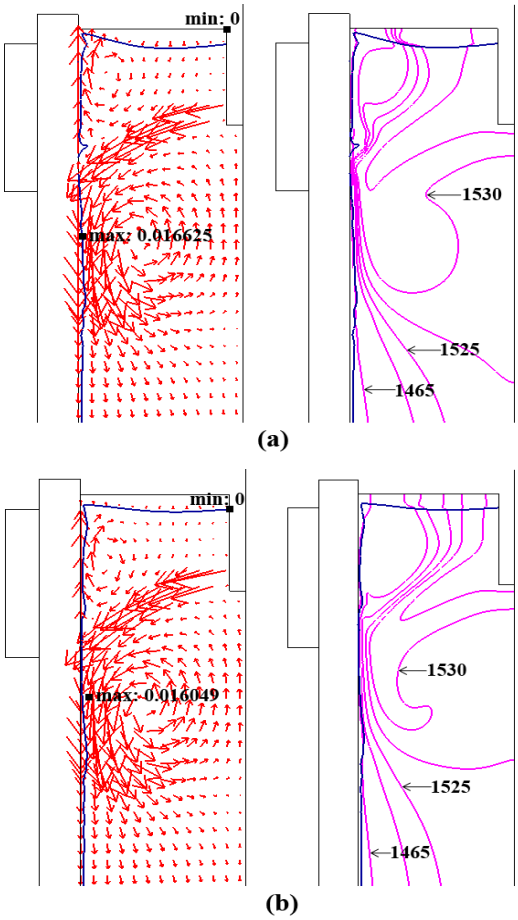

Figure 4: Influence of external current density J_s^e on two-fluid flow (first column), heat transfer and meniscus shape (second column), (a) $J_s^e = 10^4 A/m^2$; (b) $J_s^e = 5 \times 10^4 A/m^2$; (c) $J_s^e = 10^5 A/m^2$

generates a lower speed of molten steel near the mould wall and this leads to a reduction of temperature and hence the solidified steel shell is thicker. The results also show the influence of EM on the formation of oscillation marks and the meniscus shape. Figure 4(a) shows a subsurface hook on the steel surface next to the mould wall occurring at 0.08 m below the free surface and the depth of 0.005 m obtained from the mould with $J_s^e = 10^5 A/m^2$. Higher J_s^e reduces the depth of the hook and the deformation of the meniscus and the height of the meniscus. With increasing J_s^e from 10^4 to 10^5 A/m^2, the meniscus changes

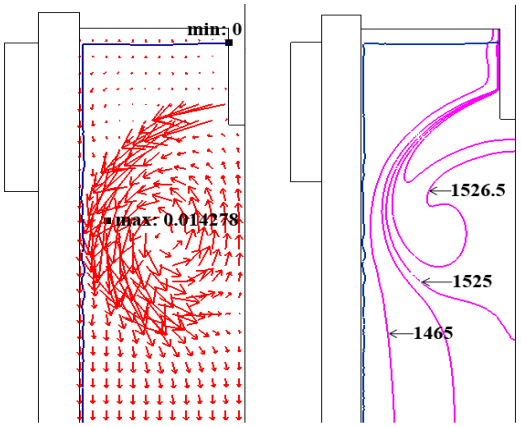

Figure 4: Continuation: Influence of external current density J_s^e on two-fluid flow (first column), heat transfer and meniscus shape (second column), (a) $J_s^e = 10^4 A/m^2$; (b) $J_s^e = 5 \times 10^4 A/m^2$; (c) $J_s^e = 10^5 A/m^2$

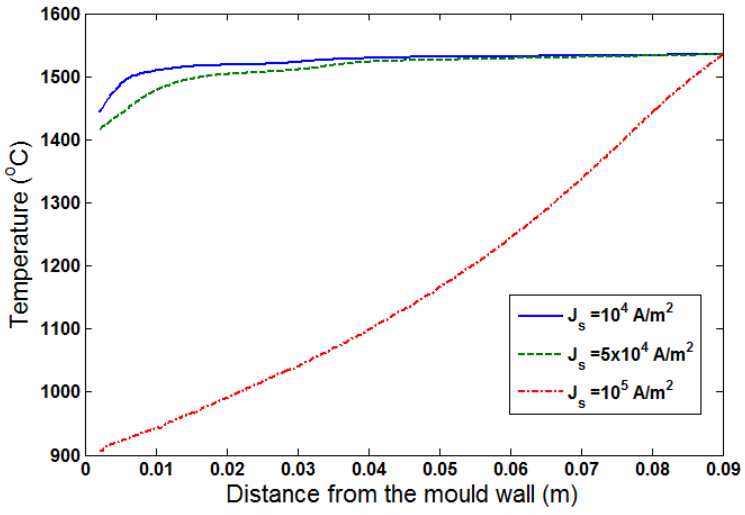

Figure 4: Influence of external current density on the temperature on the meniscus

from the parabolic shape to flat shape and the interface is more smooth as shown in Figure 4(a) − 4(c). In Figure 4(c), the meniscus may freeze speedily

to form a thicker solidified shell.

Figure 4 shows the effect of varying the source current density on the temperature profiles in the meniscus. It can be clearly seen that, with the increase of source current density, the temperature on the meniscus decreases significantly. In the case with $J_s^e = 10^5 A/m^2$, the upper flow is too weak and this causes the temperature on the upper region drops faster.

We can conclude that the EM field applied to the system has significant effect on the flow, the meniscus shape, and the temperature distribution. Using high current density, the velocity reduces and consequently the meniscus shape becomes flat and the temperature decreases. We should also emphasize that to improve the accuracy of results, the effect of mould movement must be included. Therefore, further research will be carried out to include the effect of mould movement.

Acknowledgments

The authors gratefully acknowledge the support of the Office of the Higher Education Commission and the Thailand Research Fund through the Royal Golden Jubilee Ph.D. Program (Grant No. PHD/0212/2549), and an Australia Research Council Discovery project grant.

The paper entitled "Numerical Simulation of Three-Dimensional Fluid Flow and Heat Transfer in Electromagnetic Steel Casting" published in 2009; volume 52: page 373-390 is also supported by the above sponsors.

References

[1] J. Archapitak, B. Wiwatanapataphee, Y.H. Wu, A finite element scheme for the determination of electromagnetic force in continuous steel casting, *Int. J. Comp. Numer. Anal. App.*, **5** (2004), 81-95.

[2] J. Anagnostopoulos, G. Bergeles, Three-dimensional modeling of the flow and the interace surface in a continuous casting mold model, *Metall. Mater. Trans. B*, **30B** (1998), 1095-1105.

[3] J.U. Brackbill, D. Kothe, C. Zemach, A continuum method for modeling surface tension, *J. Comp. Phy.*, **100** (1992), 335-353.

[4] Y.C. Chang, T.Y. Hou, B. Merriman, S. Osher, A level set formulation of Eulerian interface capturing methods for incompressible fluid flows, *J. Comp. Phy.*, **124** (1996), 449-464.

[5] K. Cukierski, B.G. Thomas, Flow control with local electromagnetic braking in continuous casting of steel slabs, *Metall. Mater. Trans. B*, **39B** (2007), 94-107.

[6] D. Gupta, A.K. Lahiri, Water-modeling study of surface distributes in continuous slab caster, *Metall. Mater. Trans. B*, **25B** (1993), 227-233.

[7] J.H. Jeong, D.Y. Yang, Finite element analysis of transient fluid flow with free surface using VOF (volume-of-fluid) method and adaptive grid, *Int. J. Numer. Meth. Fluids*, **26** (1998), 1127-1154.

[8] T. Li, S. Nagaya, K. Sassa, S. Asai, Study of meniscus behavior and surface properties during casting in high-frequency magnetic field, *Metall. Mater. Trans. B*, **26B** (1994), 353-358.

[9] R. Miranda, M.A. Barron, J. Barreto, L. Hoyos, J. Gonzales, Experimental and numerical analysis of the free surface in a water model of a slab continuous casting mold, *ISIJ Int.*, **45** (2005), 1626-1635.

[10] H. Nakata, J. Etay, Meniscus shape of molten steel under alternating magnetic field, *ISIJ Int.*, **32** (1992), 521-528.

[11] F. Negrini, M. Fabbri, M. Zuccarini, E. Takeuchi, M. Tani, Electromanetic control of the meniscus shape during casting in a high frequency magnetic field, *Ener. Conv. Manag.*, **41** (2000), 1687-1701.

[12] H. Oka, K. Ishii, Numerical analysis on the motion of gas bubbles using level set method, *J. Phy. Soc. Japan*, **68** (1999), 823-832.

[13] S. Osher, J.A. Sethian, Fronts propagating with curvature-dependent speed: Algorithms based on Hamilton-Jacobi formulations, *J. Comp. Phy.*, **79** (1988), 12-49.

[14] K. Schwerdtfeger, H. Sha, Depth of oscillation marks forming in continuous casting of steel, *Metall. Mater. Trans. B*, **31B** (2000), 813-826.

[15] M. Sussman, P. Smereka, S. Osher, A level set approach for computing solutions to incompressible two-phase flow, *J. Comp. Phy.*, **114** (1994), 146-159.

[16] K. Takatani, Effects of electromaghetic brake and meniscus electromanetic stirrer on transient molten steel flow at meniscus in a continuous casting mold, *ISIJ Int.*, **43** (2003), 915-922.

[17] E. Takeuchi, J.K. Brimacombe, The formation of oscillation marks in the continuous casting of steel slabs, *Metall. Mater. Trans. B*, **15B** (1984), 493-509.

[18] A. Theodorakakos, G. Bergeles, Numerical investigation of the interface in a continuous steel casting mold water model, *Metall. Mater. Trans. B*, **29B** (1997), 1321-1327.

[19] T. Toh, E. Takeuchi, M. Hojo, H. Kawai, S. Matsumura, Electromagnetic control of initial solidification in continuous casting of steel by low frequency alternating magnetic field, *ISIJ Int.*, **37** (1997), 1112-1119.

[20] Y. Watanabe, A. Saruwatari, D.M. Ingram, Free-surface flows under impacting droplets, *J. Comp. Phy.*, **227** (2008), 2344-2365.

[21] Y.H. Wu, B. Wiwatanapataphee, Modelling of turbulent flow and multiphase heat transfer under electromagnetic force, *Disc. Cont. Dyn. Sys. B*, **8** (2007), 695-706.

[22] Z. Yu, L.S. Fan, Direct simulation of the buoyant rise of bubbles in infinite liquid using level set method, *The Canadian J. Chem. Eng.*, **86** (2008), 267-275.

[23] Y. Zhang, Q. Zou, D. Greaves, Numerical simulation of free-surface flow using the level-set method with global mass correction, *Int. J. Numer. Meth. Fluids*, **29** (2009), 657-684.

[24] H.K. Zhao, B. Merriman, S. Osher, L. Wang, Capturing the behavior of bubbles and drops using the variational level set approach, *J. Comp. Phy.*, **29** (2009), 657-684.

[25] X.R. Zhu, R.A. Harding, J. Campbell, Calculation of the free surface shape in the electromagnetic processing of liquid metals, *Appl. Math. Model.*, **21** (1997), 207-214.